



# Encounters in star clusters and survival probabilities for planets

Enrico Maraboli<sup>a</sup>, Fabio Mantegazza<sup>b</sup>, Giuseppe Lodato<sup>c</sup>

Department of Physics, Università degli Studi di Milano, Via Celoria 16, Milan 20133, Italy

Received: 1 November 2022 / Accepted: 24 January 2023  
© The Author(s) 2023

**Abstract** The stability of young planetary systems is strongly influenced by multiple factors, both internal and external. In this paper, we investigate the link between the environment in which young stars form and the possibility of having stable planetary systems around them. We analyze the robustness of such systems after an encounter with another star within the same stellar cluster. We employ a model for the star cluster to extract the encounter properties, such as the mass of the perturber star and its velocity. We perform numerical simulations on systems with a single planet perturbed by an external star, in order to calculate the emission probabilities of the planet. We also calculate analytically the stellar encounter rates in the cluster. We find that such probabilities are strongly dependent on the thermal velocity of the cluster. We also notice that these probabilities are generally quite small, below 3% for the systems tested by us.

## 1 Introduction

Star clusters are one of the possible birthplaces of stars, and dynamical interactions between young stars may significantly affect the early life of its members. However, stars are not the only component of young star clusters: While in its earliest phases a large gas reservoir is also present, we also expect young stars to host planetary systems. In this paper, we explore the behavior of the planetary population which forms around the cluster members and its relation to the environment. The crowded nature of these structures brings cluster stars to experience more or less close encounters between them (for a sample of existing literature, see [1–6]). Besides the dynamical effects that encounters have in the evolution of the cluster itself, such as thermal equilibrium and relaxation, we are interested in the consequences that a close encounter between stars may have on a bound planetary system. Such encounters, indeed, can undermine the stability and even the very existence of a planetary system. Stellar encounters could occur while planets are still forming: for a review on this topic, see [7]. A consistent theory for exoplanetary population in star clusters should also include the effect of stellar fly-bys.

These phenomena are crucial for several reasons. Firstly, if a very low survival probability emerges from these kind of studies, this would challenge the apparent ubiquity of planetary systems in the Galaxy (see, e.g., [8]). Also, planetary ejections through fly-bys can be the origin of free floating planets and InterStellar Objects (ISOs). Up to now, only two ISOs were observed, I1/Oumuamua [9] and I2/Borisov [10] and their origin can be considered within the perspectives of stellar fly-bys on planetary systems [11].

In recent years, the Atacama Large Millimeter Array (ALMA) has revealed that young stars surrounded by a disk often display significant substructure in the disk morphology at a distance of  $\approx 100$  au from the star, which are typically interpreted as the effect of the presence of a planet [12]. The origin of these substructures is still under debate, and they can be due to several other factors, such as stellar encounters or dead zones. In this paper, we assume that these structures are due to the presence of planets. Such young planet population is thus relatively weakly bound to their host star and may thus be more susceptible to ejection due to stellar fly-bys.

The aim of the present paper is to analyze the frequency of close stellar fly-bys inside star clusters and determine the survival probability of a (weakly bound) planet after such an event. We also find a relation between the property of the cluster and the planetary ejection rate, in order to provide a general guideline to describe the outcome of an encounter.

---

Focus Point on Environmental and Multiplicity Effects on Planet Formation

Guest editors: G. Lodato, C.F. Manara.

<sup>a</sup> e-mail: [enrico.a.maraboli@gmail.com](mailto:enrico.a.maraboli@gmail.com) (corresponding author)

<sup>b</sup> e-mail: [fabiomanto99@gmail.com](mailto:fabiomanto99@gmail.com) (corresponding author)

<sup>c</sup> e-mail: [giuseppe.lodato@unimi.it](mailto:giuseppe.lodato@unimi.it) (corresponding author)

The paper is organized as follows: in Sect. 2, we describe the statistical and dynamical methods used in this work; in Sect. 3, we present and discuss our main results; in Sect. 4, we draw our conclusions.

## 2 Methods

Our methodology consists of the following steps. We consider a “target” young planetary system, composed of a host star and one single planet in a relatively weakly bound orbit (consistent with the expected population of young planets from ALMA studies). Then, we construct an ensemble of orbital properties for a second star (the “perturber”), by extracting them through Montecarlo sampling from a thermal distribution of stars within a star cluster of known physical parameters. For each of the encounter parameters considered, we evolve a three-body simulation involving the “target” star-planet system and the perturber. After the fly-by, we compute the orbital elements of the planet with respect to its host star and thus determine ejection and retention rates.

### 2.1 Modeling the stellar cluster

We assume that the stellar cluster is described using the Plummer model [13], a simple and spherically symmetric model (see, e.g., [1, 6, 14]). The density profile is thus given by:

$$\rho(R) = \frac{3M_{\text{cl}}}{4\pi R_0^3} \frac{1}{[1 + (R/R_0)^2]^{5/2}}, \quad (1)$$

where  $R$  is the distance from the centre of the cluster,  $M_{\text{cl}}$  is the cluster mass and  $R_0$  is a scale radius connected to the half mass radius as  $R_h \approx 1.305R_0$  and to the cluster core radius as  $R_c = R_0/\sqrt{2}$ . Considering the cluster in virial equilibrium, the thermal velocity of the stars is given by [5]:

$$v_T = \left( \frac{3\pi GM_{\text{cl}}}{32R_0} \right)^{1/2}, \quad (2)$$

which provides a typical scale for the speed of the stars in the cluster. The stellar masses are drawn from the initial mass function of Kroupa [15], with a minimum mass of  $0.015M_\odot$ . We did not set an upper limit since the distribution rapidly decrease for higher masses, so the probability to extract an extremely massive star is negligible. The initial velocity  $v_\infty$  of the perturber at infinity, where the gravitational interaction with the host system is negligible, is drawn from a Maxwell–Boltzmann distribution

$$f(v_\infty) := \frac{dP(v_\infty)}{dv_\infty} = \sqrt{\frac{6}{\pi}} \frac{3v_\infty^2}{v_T^3} \exp\left(-\frac{3v_\infty^2}{2v_T^2}\right). \quad (3)$$

Here, to use the Maxwell–Boltzmann distribution, we assumed that the cluster is virialized but not relaxed, an hypothesis that needs to be tested. To this effect, we calculate the relaxation and evaporation time of the cluster and assume that our model is valid for times shorter than the cluster relaxation time. A rough estimate of the relaxation time  $\tau_{\text{relax}}$  is given by (see [5])

$$\tau_{\text{relax}} \approx \frac{0.1N}{\ln N} \tau_{\text{cross}}, \quad (4)$$

where  $N$  is the number of stars in the cluster and the crossing time  $\tau_{\text{cross}}$  follows from

$$\tau_{\text{cross}} \approx \frac{2R_c}{v_T}. \quad (5)$$

The values of these times for the different clusters considered here are reported in Tables 3 and 4.

We have constructed several different realizations of the model, by varying the cluster properties (its mass and radius). The cluster mass and the cluster core radius (and so the parameter  $R_0$ ) are not independent, but we chose them in order to qualitatively follow a power-law fit that we have extrapolated from the observed cluster properties as reported in [16] (we excluded from the fit the sub-cluster of the Trapezium, because it is an outlier and we chose to focus on more regular clusters). We have interpolated the data using the formula

$$\frac{M_{\text{cl}}}{M_\odot} = \alpha \left( \frac{R_c}{1\text{pc}} \right)^\beta \quad (6)$$

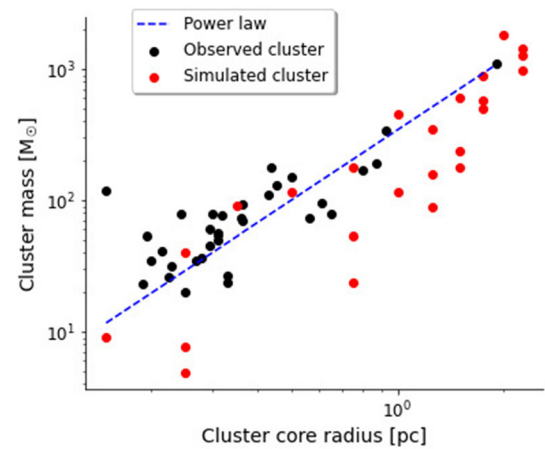
and the parameters of the fit are these:

$$\alpha = 345 \pm 17, \quad (7)$$

$$\beta = 1.784 \pm 0.080. \quad (8)$$

The fit and the data from the article are reported in Fig. 1, where we plot also the simulated parameters for the clusters. We report in Tables 3 and 4 the values of the different parameters used in the simulations.

**Fig. 1** Cluster mass as a function of the cluster core radius. Black points are observed clusters from [16], red points indicate the model clusters employed here. The dashed line is a fit of the observed points



### 2.2 Encounter rates and total number of encounters

In order to estimate the encounter rates and the total number of encounters in an open cluster, we use a cross-section argument. We define the cross section  $\sigma$  for two stars having a relative velocity at infinity  $v_\infty$  and pericenter  $R_p$ . The cross section can be written as (see [1, 17, 18]):

$$\sigma = 2\pi R_p^2 \left( 1 + \frac{GM_{\text{tot}}}{R_p v_\infty^2} \right), \tag{9}$$

where  $M_{\text{tot}}$  is the total mass of the two stars and the second term in brackets expresses gravitational focussing.

We can now write the total number of encounters  $N_{\text{enc}}$  within a given time  $\tau$  as

$$N_{\text{enc}} = \int_0^\tau n\sigma \bar{v} dt \approx n\sigma \bar{v}\tau, \tag{10}$$

where in the last equality we have considered the terms in the integral to be independent on time (an assumption that will be discussed below),  $n$  is the number density of the Plummer sphere at the core radius and  $\bar{v}$  is the mean velocity of the encounter, which will be set to  $v_T$ .

The encounter rate is thus given by (where we set also  $v_\infty = v_T$ )

$$f = \frac{N_{\text{enc}}}{\tau} \approx 3 \cdot 10^{-3} \left( \frac{N}{10^3} \right)^{3/2} \left( \frac{R_c}{1\text{pc}} \right)^{-7/2} \left( 1 + 2.152 \left( \frac{M_{\text{tot}}}{M_\odot} \right) \left( \frac{R_c}{1\text{pc}} \right) \right) \left( \frac{N}{10^3} \right)^{-1} \text{My}^{-1}. \tag{11}$$

The typical encounter timescale is  $T = 1/n\sigma\bar{v}$ . In the limit where gravitational focussing dominates ( $GM_{\text{tot}}/R_p \gg v_\infty^2$ ), we thus obtain the following estimate for  $T$ :

$$T \approx 37\text{My} \left( \frac{100\text{pc}^{-3}}{n} \right) \left( \frac{v_\infty}{1\text{km/s}} \right) \left( \frac{10^3\text{au}}{R_p} \right) \left( \frac{M_\odot}{M_{\text{host}}} \right). \tag{12}$$

The result above is in good agreement with the result reported in [4, 19].

The result above is affected by many approximations, which will be discussed below, that limit the validity of the obtained results to the early stages of life of the open clusters, before the relaxation. It is also interesting to note that, as reported in Table 6 in Appendix, in the various clusters almost no star experienced a close fly by (with pericenter smaller than 1000 au) before the relaxation time. We will discuss all these results in the next sections.

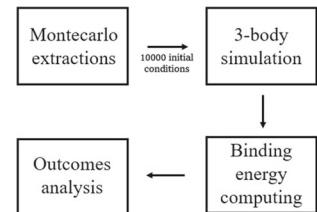
### 2.3 Encounters in planetary systems

We choose a set of five model planetary systems composed by a star and a single orbiting planet, in order to investigate their differences in terms of emission rates. We built a ‘‘Standard’’ system, with a host mass of  $1M_\odot$  a planet mass of  $1M_{\text{Jup}}$  (Jupiter mass) at a distance of 100 au, while the other four have parameters corresponding to existing stars with hints of having young planets at large distances, based on dust morphologies observed with ALMA. Their fundamental characteristics are listed in Table 1.

**Table 1** List of all planetary systems studied ([12, 20–22]).

System	$M_{\text{host}} (M_{\odot})$	$M_{\text{planet}} (M_{\text{Jup}})$	Distance (au)	System energy (km/s)
Standard	1	1	100	2.10
RY Tau	$2.04^{+0.3}_{-0.26}$	0.077	$43.41 \pm 0.13$	4.57
CIDA 1	$\approx 0.1$	$\approx 0.5$	$\approx 12$	1.92
HD 143006	$1.5^{+0.1}_{-0.1}$	23	22	5.50
GO Tau	$0.48^{+0.01}_{-0.01}$	0.057	$58.91 \pm 0.66$	1.90

We indicate the host mass as  $M_{\text{host}}$  and the planet mass as  $M_{\text{planet}}$ . The system energy is the binding energy per reduced mass unit of the respective two body system

**Fig. 2** Flowchart of the code

First of all, we choose to consider as encounters, according to the current literature too (see, e.g., [2]), events in which the perturber reaches a pericentre distance below 1000 au. Consequently, we compute the distribution of the pericentres between 0 and 1000 au from the cross-section argument. It reads

$$\frac{dP(r_p)}{dr_p} = \frac{2r_p + GM_{\text{tot}}/v_{\infty}^2}{(R_p^{\text{max}})^2 + GR_p^{\text{max}}M_{\text{tot}}/v_{\infty}^2}, \quad (13)$$

where  $P(r_p) = N_{\text{enc}}(r_p, t)/N_{\text{enc}}(R_p^{\text{max}}, t)$ ,  $r_p$  is the pericentre distance and  $R_p^{\text{max}} = 1000$  au.

The orbital properties of the encounter, including the perturber mass and relative velocity, are instead randomly selected according to the chosen cluster features (as described above). Then we extract the three angles that determine the relative inclination of the perturber orbit with respect to the orbital plane of the planet. The distribution of inclination  $I$  is uniform in the variable  $\cos I$ , with  $I \in [0, \pi]$ , while the distributions of the longitude of the ascending node  $\Omega$  and the argument of pericentre  $\omega$  are uniform in  $\Omega$  and  $\omega$ , with  $\Omega \in [0, 2\pi)$  and  $\omega \in [0, \pi)$ . Finally, we draw the pericentre distance  $r_p$  from the distribution (13) and  $v_{\infty}$  from the velocity distribution described in Sect. 2.1.

#### 2.4 Numerical simulations

We tested our planetary systems with a wide variety of star clusters. We generated several different clusters, all of them through the Plummer model described in Sect. 2.1, and we extracted 10,000 initial conditions for each of them. We report the characteristics of these clusters and their details in Appendix A.

We define the beginning of the encounter by setting the initial distance of the perturber to 5000 au, since the planet-perturber potential energy can be safely neglected with respect to the host-planet one at such a distance. The end of the encounter, and consequently of the single numerical simulation, happens when the perturber reaches a distance of 5000 au from the host again. The initial velocity of the perturber is set equal to  $v_{\infty}$ .

We solve the three-body problem via standard integration techniques. We developed a code which employs a leapfrog method of integration [23], since it is a symplectic second-order algorithm. We report a flowchart of the code in Fig. 2. In order to numerically determine the outcome of an encounter, we computed at the end of each simulation the host-planet binding energy and the perturber-planet binding energy, assuming that these two couples were two independent two-body systems. We can safely make this hypothesis, since the host and the perturber stand at a very large distance at the end of a simulation (5000 au). Hence if the host-planet energy is *negative*, the planet is considered to be still bound to the host; if the host-planet energy is *positive*, the planet is considered to be torn away from the host. This is what we call *emission*. If the planet-perturber system energy is *negative*, the planet is considered to be captured by the perturber. We tested the stability and the precision of our code on particular two-body systems with very high eccentricities. We adopt a softening parameter for all the three bodies, which is set to  $\varepsilon = 0.005$  au.

**Table 2** Numerical values of fit coefficients  $A, B$  with their errors  $\sigma_A, \sigma_B$

System	$A$	$\sigma_A$	$B$	$\sigma_B$
Standard	0.009	0.001	0.0235	0.0007
RY Tau	0.0012	0.0007	0.0052	0.0004
CIDA 1	0.0111	0.0008	0.0151	0.0005
HD 143006	0.0022	0.0005	0.0073	0.0003
GO Tau	0.014	0.002	0.027	0.001

### 3 Results and discussion

The main result we present in this paper is the direct connection between emission rates and cluster thermal velocities. We define the emission probability  $P_{em}$  as  $P_{em} = N_{em}/N_{tot}$ , where  $N_{em}$  is the total number of emission found for a single set of initial conditions and  $N_{tot} = 10,000$  is the total number of encounters simulated for each set of initial conditions. We found a linear power law correlation between the emission probability and the cluster thermal velocities:

$$P_{em}(v_T) = -A \cdot \frac{v_T}{1 \text{ km/s}} + B. \tag{14}$$

In Table 2, we list the fitted values for the coefficients  $A, B$  and their uncertainties  $\sigma_A, \sigma_B$ . As we can see in Fig. 3 too, the emission probabilities are quite low: the highest of them is around 2.7% for the *GO Tau* system. We obtain that the mean value of the pericentre distribution is roughly 500 au. The pericentre distribution itself grows monotonically, leaving few perturbers within the 500 au threshold. This is probably the main cause of the lack of emissions, since the tested planets orbit their star no further than 100 au. Another relevant aspect that surely influenced this outcome is the mass distribution of the perturber. The Kroupa IMF [15] indeed has a mean value of  $0.46M_{\odot}$ , generally lower than the host mass. The rareness of (sufficiently) high mass perturbers combined with the lack of very close encounters hence leads to generally low emission probabilities for all the tested systems, independently from their binding energy.

The dynamical argument standing behind the dependence on thermal velocity is the effective time scale during which linear momentum can be transferred from the perturber to the planet. If we consider the planet as a test particle, then we can neglect the momentum transferred from the planet to the perturber. We can justify this approximation by noticing that the ratio between the planet mass and the perturber mass sits always below  $10^{-2}$ . From the definition of the momentum change  $\Delta \vec{p}$ , we can immediately write the following inequalities:

$$0 \leq |\Delta \vec{p}(t)| = \left| \int_{t_0}^t \vec{F}_{pp}(\vec{r}) dt' \right| \leq \int_{t_0}^t |\vec{F}_{pp}(\vec{r})| dt'. \tag{15}$$

where  $\vec{F}_{pp}(\vec{r})$  is the perturber gravitational pull acting on the planet and  $t$  is the time passed since the instant  $t_0$  in which the encounter begins. Inequality (15) states that a longer fly-by time allows a larger interval for  $|\Delta \vec{p}(t)|$  to span during the encounter. Hence raising the momentum transferred  $|\Delta \vec{p}(t)|$  threshold could become crucial for a planet in order to overcome the host escape

**Fig. 3** Emission probability as a function of thermal velocity  $v_T$  for all planetary systems. The coloured dots represent the data points we obtained for each planetary system, while the solid lines are the respective best fit lines for them

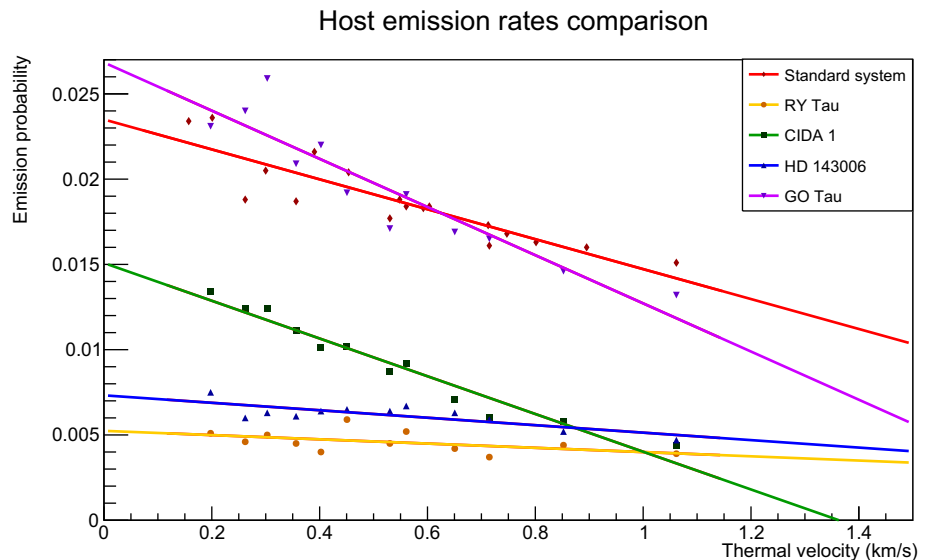
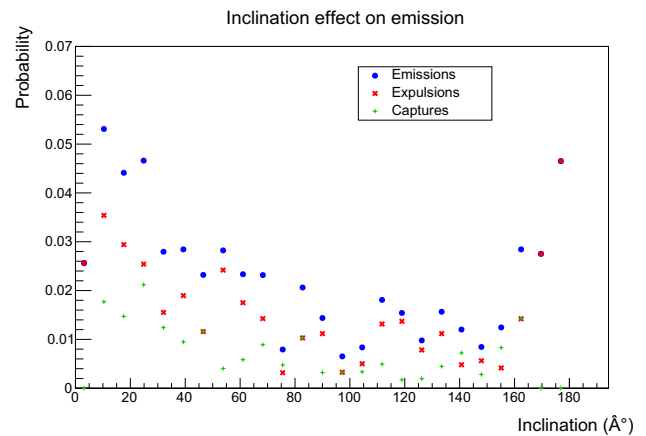


**Fig. 4** The effect of inclinations on emission events. We named “expulsion” an emission event in which the planet, after the encounter, is gravitationally unbound from both the host and the perturber. We named “capture” an emission event in which the planet leaves its host star and it is captured by the perturber. The amount of emissions is the sum of expulsion and capture events number. An inclination of 0° corresponds to a fully prograde encounter, vice versa an inclination of 180° stands for a fully retrograde encounter



velocity. Furthermore, the fly-by duration is directly related to the initial velocity  $v_\infty$  and consequently to  $v_T$ . A high  $v_T$  indeed allows encounters with a high  $v_\infty$  (and a small interaction time) to happen more frequently. Vice versa, a low  $v_T$  makes rare rapid encounters, allowing more planets to escape their hosts.

We present in Fig. 4 a relation between emission rates and the inclination angle  $I$ . This relation is taken from the dataset of the Standard system at low thermal velocity, where emissions are more abundant. Similar results are found for the other tested systems. We can easily expect higher emission rates for prograde encounters, since the relative velocity between the planet and the perturber is lower, and consequently, it is easier to transfer momentum to the planet. Unexpectedly, we find a rise of probabilities for retrograde events. However, the available statistic for these events is still low to ensure that this is a real feature of encounters. We think that this rise is caused by two (or more) consecutive encounters between the planet and the perturber, where the first encounter triggers the second. This behavior of planetary systems on retrograde encounters can be an interesting topic for future papers.

The second main result we report is the calculation of the encounter rates in an open star cluster and the probability that an encounter between a star from the star cluster, and an host system leads to an emission of the planet orbiting around the latter one. This probability is simply calculated by multiplying the encounter rates by the emission rates presented before. For the encounter rates, in Appendix B we report all the encounter rates  $f$  calculated for the parameters of the different simulations, while in Fig. 5 we plot the rates  $f$  as a function of the cluster core radius and of the different number of stars in the cluster.

Instead of reporting the results found for the simulation, which are strongly dependent on the chosen cluster parameters, we focus on presenting the values that are compatible with the correlation between mass and core radius found in Sect. 2.1. As it can be seen, there are not many differences and the encounter rates goes from  $\approx 1$  encounter every Myears, for very dense clusters, to 1 encounter every hundreds Myears, for the less dense clusters.

We finally notice the existence of a relation between emission rates and the mean eccentricity of the perturbers. We observe decreasing emission rates as the mean eccentricity rises. This behavior is also related to the role of thermal velocity. In a two-body hyperbolic orbit, the eccentricity  $e$  is related to the encounter velocity as

$$e = 1 + \frac{r_p v_\infty^2}{G(M_1 + M_2)}. \tag{16}$$

The quadratic dependence from  $v_\infty$  explains, through its distribution, the role of thermal velocity in the emission-eccentricity relation. A bit of information here is added by the contribution of the pericentre distance  $r_p$ , which can occasionally balance the  $v_\infty$  term. We also find, unsurprisingly, that the emission probability grows with the perturber mass and it is decreasing with the pericentre distance, as depicted in Fig. 6.

### 3.1 Discussion of results

Let us start discussing the approximations done, and how they influenced the results. First of all, we assumed the cluster to be in virial equilibrium, this is a sensible approximation since the time it takes for the cluster to virialize is much shorter than the relaxation time. For the distribution of the speed at infinity, we used a Maxwell–Boltzmann distribution, which would assume a high frequency of encounters/interactions between the stars in the cluster with respect to the relaxation time. Now, this hypothesis, *a posteriori*, is not verified so the only thing we can assume is that the distribution of the speeds is not very different from the Maxwell–Boltzmann one. However, assuming a quasi-virialized velocity distribution does not affect our results heavily. Since we found a relation between thermal velocities and emission rates, for a quasi-virialized cluster it will be sufficient to compute an “effective” thermal velocity from the virial theorem (see [5]) in order to use such relation and obtain a corrected result.

Secondly, in order to describe the density profile of the cluster, we used the Plummer model, which does not contain a time dependence and does not take in consideration relaxation effects.



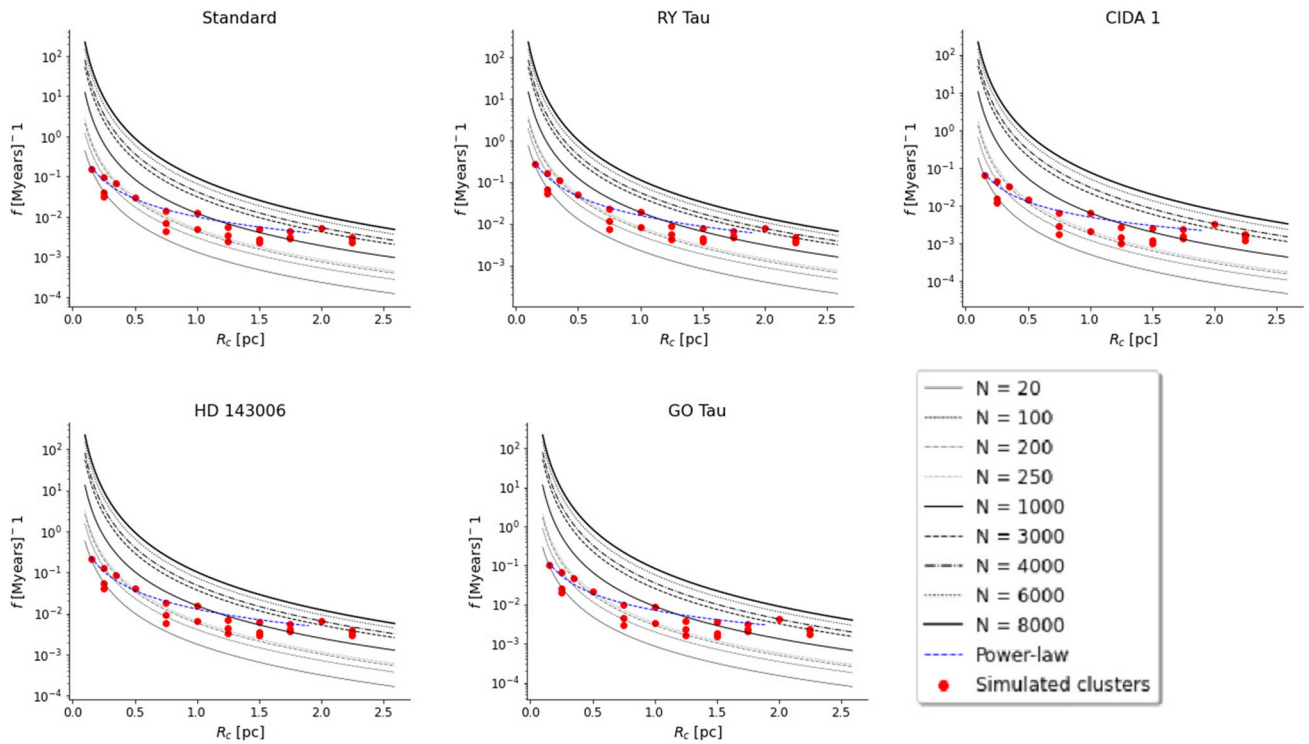


**Fig. 5** Encounter rates for every host system, they are sorted from the left to the right and from the top to the bottom.  $N$  is the number of stars in the cluster, the blue dashed line is the power law fit presented in eq. (6) and the red dot are the simulated clusters, which parameters are reported in Tables 3 and 4

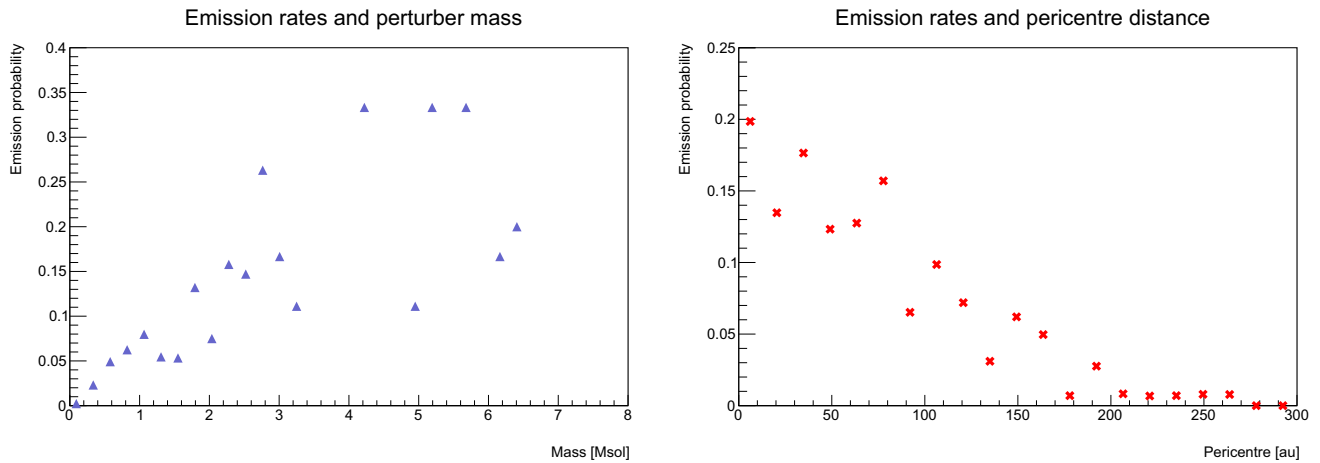
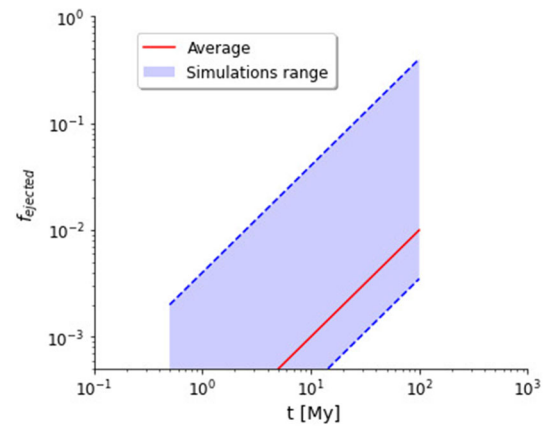


**Fig. 6** On the left panel, we draw an example, taken from GO Tau dataset, of the dependence of emission probabilities on the mass of the perturber. On the right panel, instead we report an example, taken from Standard system dataset, of the dependence of emission probabilities on the pericentre of the perturber. Similar results are found for the other systems

Furthermore we can see that, since we have no time dependencies in eq. (10), the rate is constant and so the number of encounter increases linearly with time, which can not be true due to cluster relaxation mechanisms and as shown trough N-body simulations (see [1] for example). These are the main reasons for which we can assume that our results are valid only during the early stages of life of the cluster and before the relaxation. Obviously, more accurate assumption should be done in order to predict the rates of encounter valid also after the relaxation. For example, we could insert a time dependence in the mass density of the cluster following the values found in [24]. Another way to consider the relaxation effects could be to consider a cross section dependent on the number of encounters: This could be an interesting topic for further studies.

Another aspect that deserves to be discussed is the possibility of having more than a single planet (or star!) in the considered planetary system. In our work, we do not consider these possibilities too, but we can make a comparison with the existing literature. We refer to the work by Li et al. [25] for the effects of the presence of binaries in the considered clusters. It is shown how binary systems are much more effective in triggering the emission of a planet from its host star. On the planetary side, the case of multiplanetary

**Fig. 7** Fraction of emitted planets as a function of the time (the range of the axes is chosen to ease the comparison with Fig. 7, Model w3-1d, of the work [6]). The blue region represents the range of possible values obtained from the simulations. The red line is a rough estimate of the average values found in the simulations



systems has been explored by Davies et al. [1], who consider the behavior of four giant planets after a close stellar fly-by. Here planet-planet scattering phenomena acquire great importance after the encounter, eventually leading the system to disruption. But when these effects of mutual planet interaction are negligible, which happens when the encounter is grazing, they find a fraction  $f_{\text{ion}}$  of immediately ejected planet of  $\approx 1\% - 3\%$ , consistent with our results.

We can provide a check of our results through the work of Fujii and Hori [6]. We approached semi-analytically the encounter rate problem, and we explored numerically the effective encounter dynamics. Vice versa, Fujii and Hori made numerical simulations for the cluster dynamics and determined through semi-analytical methods the outcome of close star encounters. We found a range of values for the rates of emission of a planet through the quantity  $f_{\text{ejected}}$ , defined as follows:

$$f_{\text{ejected}} = f P_{\text{em}} t, \quad (17)$$

where  $t$  is the time passed since the birth of the cluster. The result is reported in Fig. 7, which has to be compared with Fig. 7, model w3-1d, of Fujii and Hori [6]. There is a large variability in our results, because the host-planet distance varies for each planetary system and we simulate clusters with different parameters. Anyway, our results describe low-density clusters (according to the distinction made in [6]) and, remembering Table 1, we are interested in the fraction of emitted planets with distance from the star between 10 and 100 au. Hence we obtained from Eq. 17 a range of values, in which we highlight the average fraction. Fujii and Hori for this kind of planetary systems find  $f_{\text{ejected}} \approx 10^{-3}$  at 10 Myr, and their emission rates for planets with distance from the star between 10 and 100 au are well placed into our simulations range of Fig. 7. We can state that there is a significant overlap between our results and the one reported in the article.

In summary, our results are consistent with the existing stellar cluster based planet formation studies and they add more quantitative information to be compared with [1, 3, 4, 6].

#### 4 Summary and conclusions

We have modeled a series of star clusters, according to the observed power law in [16], in order to obtain the encounter rates between stars. For each cluster, we used the Plummer model [13] and the initial mass function (IMF) from Kroupa [15], while we varied the core radius and the number of stars. Our models and approximations provided those values for a limited time interval over the clusters lifetime. We indeed refer our results to the early times after the clusters formation, safely before that the relaxation time occurs. From each cluster we inferred the distribution of velocities and the distribution of pericenters in order to perform numerical simulations of the encounters. We employed a wide set of clusters for each tested system: we wanted indeed to sample as better as we could a realistic interval of thermal velocities. This interval is once again derived from the data in [16], reported in Fig. 1, using Eq. 2. We tested five different planetary systems, each one underwent 10,000 encounters with fellow cluster members.

- 1 We found encounter rates that span between 1 encounter/Myr, for high density clusters, to  $\approx 10^{-2}$  encounters/Myr, for very low density clusters. Our method led to a result that is in good agreement with the work by Pfalzner [4].
- 2 From the numerical simulations performed, we obtained the emission rates (or survival probabilities) for a sample of planetary systems. The emission probability for a single encounter we found is generally small, below 3%, hence a single planet has quite a high probability to survive after a close encounter. Planetary systems with more than a single planet involve further complications than the single perturber pull: Davies et al. [1] investigated this branch of the problem. They also found a fraction  $f_{\text{ion}}$  of immediately ejected planets that is in good agreement with our results, since in an immediate emission event we can neglect the effects of planet-planet scattering.
- 3 We observed a direct relation between emission rates and the thermal velocity of the considered clusters. This relation can be expressed as a linear power law for all the tested systems: Hence we saw how the environment can influence his own planetary



population. Comparing emission rates with the mean eccentricity provides an indirect way to see this relation and adds the contribution of the pericentre distance. We also checked that parameters such as the perturber mass, the pericentre distance or the perturber inclination influence the encounter outcome in the usually expected way.

In summary, we studied the relation between a planetary system and its external environment by directly testing the environment influence on the actual encounters. We saw how this environment affects the planetary populations hosted and the timescales on which this process acts. Our numerical approach allows to compute the emission probabilities with an accuracy that is way better than through the existing semianalytical methods. Further studies may enlighten some aspects we neglected or improve the approximations we made. A worthy advance could be made by studying the behavior of emission rates after the cluster relaxation and the differences with the early times here analyzed. Still on the early times of the cluster, it could be improved this study by picking a non-equilibrium velocity distribution for the stars. It could also be interesting to investigate more thoroughly the dynamics of the fully retrograde encounter, checking if it effectively leads to a rise of emissions.

**Funding** Open access funding provided by Università degli Studi di Milano within the CRUI-CARE Agreement.

**Data Availability Statement** This manuscript has associated data in a data repository. [Authors’ comment: All the extracted initial conditions we employed to simulate the encounters in this paper are available from the authors upon request. The results of the encounters simulations too are available from the authors upon request through the reported contacts].

**Open Access** This article is licensed under a Creative Commons Attribution 4.0 International License, which permits use, sharing, adaptation, distribution and reproduction in any medium or format, as long as you give appropriate credit to the original author(s) and the source, provide a link to the Creative Commons licence, and indicate if changes were made. The images or other third party material in this article are included in the article’s Creative Commons licence, unless indicated otherwise in a credit line to the material. If material is not included in the article’s Creative Commons licence and your intended use is not permitted by statutory regulation or exceeds the permitted use, you will need to obtain permission directly from the copyright holder. To view a copy of this licence, visit <http://creativecommons.org/licenses/by/4.0/>.

### Appendix A: Further simulated clusters

Here we report all the clusters employed to fit the power law in Eq. (14). We managed to generate them in order to span properly the range of thermal velocities between 0 and 1 km/s.

We produced eighteen clusters for the Standard system. Their characteristics are listed in Table 3.

Finally, for the other four systems (RY Tau, CIDA 1, HD143006, GO Tau) we generated twelve clusters, which are listed in Table 4.

**Table 3** The eighteen clusters generated for the Standard system

ID	$N$	$M (M_{\odot})$	$R_c$ (pc)	$v_T$ (km/s)	$\tau_{cross}$ (Myr)	$\tau_{relax}$ (Myr)
1	20	9.2	0.15	0.262	1.12	0.75
2	200	92	0.35	0.561	1.22	4.61
3	250	115	0.5	0.530	1.85	8.36
4	250	115	1	0.356	5.50	24.89
5	1000	460	1	0.714	2.74	39.68
6	4000	1840	2	1.062	3.69	177.73
7	100	40.6	0.25	0.454	1.08	2.12
8	410	178.0	0.75	0.548	2.68	17.39
9	780	346.1	1.25	0.592	4.13	46.94
10	1500	601.1	1.5	0.713	4.12	74.98
11	2200	886.9	1.75	0.801	4.28	108.98
12	3200	1423.0	2.25	0.895	4.92	189.36
13	12	4.9	0.25	0.157	3.12	1.40
14	55	23.9	0.75	0.201	7.30	9.60
15	200	88.7	1.25	0.300	8.15	29.88
16	450	180.3	1.5	0.390	7.53	49.41
17	1250	503.9	1.75	0.604	5.67	88.74
18	2230	991.6	2.25	0.747	5.89	165.53

Here  $N$  is the number of stars in the cluster,  $M$  is the mass of the cluster,  $R_c$  is its core radius,  $v_T$  is the thermal velocity,  $\tau_{cross}$  and  $\tau_{relax}$  are, respectively, the crossing time and the relaxation time

**Table 4** The twelve clusters generated

ID	$N$	$M (M_{\odot})$	$R_c$ (pc)	$v_T$ (km/s)	$\tau_{\text{cross}}$ (Myr)	$\tau_{\text{relax}}$ (Myr)
1	20	9.2	0.15	0.262	1.12	0.75
2	200	92	0.35	0.561	1.22	4.61
3	250	115	0.5	0.530	1.85	8.36
4	250	115	1	0.356	5.50	24.89
5	1000	460	1	0.714	2.74	39.68
6	4000	1840	2	1.062	3.69	177.73
7b	19	7.7	0.25	0.198	2.47	1.47
8b	125	54.3	0.75	0.303	4.84	11.99
9b	360	159.7	1.25	0.402	6.085	36.11
10b	600	240.4	1.5	0.451	6.51	54.35
11b	1450	584.5	1.75	0.651	5.26	93.52
12b	2900	1289.6	2.25	0.852	5.17	182.50

Simulations from this list were performed on all of the systems in Table 1, except for the Standard system. Here  $N$  is the number of stars in the cluster,  $M$  is the mass of the cluster,  $R_c$  is its core radius,  $v_T$  is the thermal velocity,  $\tau_{\text{cross}}$  and  $\tau_{\text{relax}}$  are, respectively, the crossing time and the relaxation time

## Appendix B: Encounter rates for the different clusters

Here we report the encounter rates for the different clusters parameters and for the different host systems in Table 5 and the total number of encounters in a relaxation time in Table 6. We remind that the clusters named 7b, 8b, 9b, 10b, 11b, 12b were employed for all our simulated systems except for the Standard system. Vice versa, clusters 7, 8, 9, 10, 11, 12 were employed only for the Standard system.

**Table 5** Encounter rates for the different simulations and host system

ID	$f_{\text{Standard}}$	$f_{\text{RY Tau}}$	$f_{\text{CIDA 1}}$	$f_{\text{HD 143006}}$	$f_{\text{GO Tau}}$
1	0.158	0.266	0.064	0.210	0.104
2	0.068	0.109	0.033	0.088	0.048
3	0.031	0.049	0.014	0.040	0.021
4	0.005	0.008	0.002	0.007	0.003
5	0.012	0.019	0.007	0.015	0.009
6	0.005	0.008	0.003	0.007	0.004
7/7b	0.099	0.067	0.016	0.053	0.026
8/8b	0.014	0.012	0.003	0.009	0.005
9/9b	0.006	0.006	0.001	0.005	0.002
10/10b	0.005	0.004	0.001	0.004	0.002
11/11b	0.004	0.005	0.002	0.004	0.002
12/12b	0.003	0.004	0.002	0.004	0.002
13	0.031				
14	0.004				
15	0.002				
16	0.002				
17	0.003				
18	0.002				

All values of the encounter rates  $f$  are expressed in  $\text{Myr}^{-1}$

**Table 6** Number of encounters  $N_{\text{enc}}$  within the relaxation time  $\tau_{\text{relax}}$ 

ID	Standard	RY Tau	CIDA 1	HD 143006	GO Tau
1	0	0	0	0	0
2	0	1	0	0	0
3	0	0	0	0	0
4	0	0	0	0	0
5	0	1	0	1	0
6	1	1	1	1	1
7/7b	0	0	0	0	0
8/8b	0	0	0	0	0
9/9b	0	0	0	0	0
10/10b	0	0	0	0	0
11/11b	0	0	0	0	0
12/12b	1	1	0	1	0
13	0				
14	0				
15	0				
16	0				
17	0				
18	0				

We approximated the number of encounters to the closest integer

## References

- D. Malmberg, M.B. Davies, D.C. Heggie, The effects of fly-bys on planetary systems. *Mon. Not. R. Astron. Soc.* **411**(2), 859–877 (2011). <https://doi.org/10.1111/j.1365-2966.2010.17730.x><https://academic.oup.com/mnras/article-pdf/411/2/859/4098058/mnras0411-0859.pdf>
- D. Malmberg, M.B. Davies, D.C. Heggie, The effects of fly-bys on planetary systems. *MNRAS* **411**(2), 859–877 (2011). <https://doi.org/10.1111/j.1365-2966.2010.17730.x>. [arXiv:1009.4196](https://arxiv.org/abs/1009.4196) [astro-ph.EP]
- S. Pfalzner, L.L. Aizpuru Vargas, A. Bhandare, D. Veras, Significant interstellar object production by close stellar flybys. *Astron. Astrophys.* **651**, A38 (2021). <https://doi.org/10.1051/0004-6361/202140587>. [arXiv:2104.06845](https://arxiv.org/abs/2104.06845) [astro-ph.SR]
- S. Pfalzner, Early evolution of the birth cluster of the solar system. *A & A* **549**, A82 (2013). <https://doi.org/10.1051/0004-6361/201218792>
- J. Binney, S. Tremaine, *Galactic Dynamics*. Second Edition (2008)
- M. Fujii, Y. Hori, Survival rates of planets in open clusters: the pleiades, hyades, and praesepe clusters. *Astron. Astrophys.* **624**, A110 (2019)
- N. Cuello, F. Ménard, D.J. Price, Close encounters: How stellar flybys shape planet-forming discs (2022). [arXiv:2207.09752](https://arxiv.org/abs/2207.09752) [astro-ph.EP]
- W. Zhu, S. Dong, Exoplanet statistics and theoretical implications. *Ann. Rev. Astron. Astrophys.* **59**, 291–336 (2021). <https://doi.org/10.1146/annurev-astro-112420-020055>. [arXiv:2103.02127](https://arxiv.org/abs/2103.02127) [astro-ph.EP]
- P. Bacci, M. Mastrapieri, L. Tesi, G. Fagioli, M.P.E.C. 2017-U181. *Minor Planet Center Electronic Circulars* **2017-U181** (2017)
- G. Borisov, H. Sato, P. Birtwhistle, G. Fagioli, M.P.E.C. 2019-R106. *Minor Planet Center Electronic Circulars* **2019-R106** (2019)
- S. Pfalzner, L.L. Aizpuru Vargas, A. Bhandare, D. Veras, Significant interstellar object production by close stellar flybys. *Astron. Astrophys.* **651**, A38 (2021). <https://doi.org/10.1051/0004-6361/202140587>. [arXiv:2104.06845](https://arxiv.org/abs/2104.06845) [astro-ph.SR]
- G. Lodato, G. Dipierro, E. Ragusa, F. Long, G.J. Herczeg, I. Pascucci, P. Pinilla, C.F. Manara, M. Tazzari, Y. Liu et al., The newborn planet population emerging from ring-like structures in discs. *Mon. Not. R. Astron. Soc.* **486**(1), 453–461 (2019)
- H.C. Plummer, On the problem of distribution in globular star clusters: (Plate 8.). *Mon. Not. R. Astron. Soc.* **71**(5), 460–470 (1911). <https://doi.org/10.1093/mnras/71.5.460>. <https://academic.oup.com/mnras/article-pdf/71/5/460/2937497/mnras71-0460.pdf>
- F.C. Adams, E.M. Proszkow, M. Fatuzzo, P.C. Myers, Early evolution of stellar groups and clusters: Environmental effects on forming planetary systems. *Astrophys. J.* **641**(1), 504–525 (2006). <https://doi.org/10.1086/500393>.
- P. Kroupa, S. Aarseth, J. Hurley, The formation of a bound star cluster: from the Orion nebula cluster to the Pleiades. *Mon. Not. R. Astron. Soc.* **321**(4), 699–712 (2001). <https://doi.org/10.1046/j.1365-8711.2001.04050.x><https://academic.oup.com/mnras/article-pdf/321/4/699/3180383/321-4-699.pdf>
- C.J. Lada, E.A. Lada, Embedded clusters in molecular clouds. *Ann. Rev. Astron. Astrophys.* **41**(1), 57–115 (2003). <https://doi.org/10.1146/annurev.astro.41.011802.094844>.
- P.J. Armitage, *Astrophysics of Planet Formation*, 2nd edn. (Cambridge University Press, 2020). <https://doi.org/10.1017/9781108344227>
- W. Hao, M. Kouwenhoven, R. Spurzem, The dynamical evolution of multiplanet systems in open clusters. *Mon. Not. R. Astron. Soc.* **433**(1), 867–877 (2013)
- M.B. Davies, Turning solar systems into extrasolar planetary systems in stellar clusters. *Proc. Int. Astron. Union* **6**(S276), 304–307 (2010). <https://doi.org/10.1017/S1743921311020369>
- A. Garufi, M. Benisty, P. Pinilla, M. Tazzari, C. Dominik, C. Ginski, T. Henning, Q. Kral, M. Langlois, F. Menard et al., Evolution of protoplanetary disks from their taxonomy in scattered light: spirals, rings, cavities, and shadows. *Astron. Astrophys.* **620**, A94 (2018)
- P. Pinilla, A. Natta, C.F. Manara, L. Ricci, A. Scholz, L. Testi, Resolved millimeter-dust continuum cavity around the very low mass young star cida 1. *Astron. Astrophys.* **615**, A95 (2018)
- P. Pinilla, N. Kurtovic, M. Benisty, C. Manara, A. Natta, E. Sanchis, M. Tazzari, S. Stammer, L. Ricci, L. Testi, A bright inner disk and structures in the transition disk around the very low-mass star cida 1. *Astron. Astrophys.* **649**, A122 (2021)

23. P. Young, The leapfrog method and other symplectic algorithms for integrating newton's laws of motion. Lecture notes in University of California, Santa Cruz (2014)
24. S. Pfalzner, Universality of young cluster sequences. *A & A* **498**(2), L37–L40 (2009). <https://doi.org/10.1051/0004-6361/200912056>
25. D. Li, A.J. Mustill, M.B. Davies, Encounters involving planetary systems in birth environments: the significant role of binaries. *Mon. Not. R. Astron. Soc.* **499**(1), 1212–1225 (2020). <https://doi.org/10.1093/mnras/staa2945>. [arXiv:2008.08842](https://arxiv.org/abs/2008.08842) [astro-ph.EP]